

## Elsevier instructions for the preparation of a 1-column format camera-ready paper in L<sup>A</sup>T<sub>E</sub>X

P. de Groot<sup>a\*</sup>, R. de Maas<sup>a†</sup>, X.-Y. Wang<sup>b</sup> and A. Sheffield<sup>a‡</sup>

<sup>a</sup>Mathematics and Computer Science Section, Elsevier Science B.V.,  
P.O. Box 103, 1000 AC Amsterdam, The Netherlands

<sup>b</sup>Economics Department, University of Winchester,  
2 Finch Road, Winchester, Hampshire P3L T19, United Kingdom

These pages provide you with an example of the layout and style which we wish you to adopt during the preparation of your paper. Your text will be photographically reduced by 20–25%. This is the output from the L<sup>A</sup>T<sub>E</sub>X document class you requested.

### 1. FORMAT

Text should be produced within the dimensions shown on these pages: total width of 16 cm and a maximum length of 21 cm on first pages and 23 cm on second and following pages. The L<sup>A</sup>T<sub>E</sub>X document class uses the maximum stipulated length apart from the following two exceptions (i) L<sup>A</sup>T<sub>E</sub>X does not begin a new section directly at the bottom of a page, but transfers the heading to the top of the next page; (ii) L<sup>A</sup>T<sub>E</sub>X never (well, hardly ever) exceeds the length of the text area in order to complete a section of text or a paragraph. Here are some references: [1,2].

#### 1.1. Spacing

We normally recommend the use of 1.0 (single) line spacing. However, when typing complicated mathematical text L<sup>A</sup>T<sub>E</sub>X automatically increases the space between text lines in order to prevent sub- and superscript fonts overlapping one another and making your printed matter illegible.

#### 1.2. Fonts

These instructions have been produced using a 12 point Computer Modern Roman. Other recommended fonts are 12 point Times Roman, New Century Schoolbook, Bookman Light and Palatino.

---

\*Footnotes should appear on the first page only to indicate your present address (if different from your normal address), research grant, sponsoring agency, etc. These are obtained with the `\thanks` command.

†For following authors with the same address use the `\addressmark` command.

‡To reuse an addressmark later on, label the address with an optional argument to the `\address` command, e.g. `\address[MCS D]`, and repeat the label as the optional argument to the `\addressmark` command, e.g. `\addressmark[MCS D]`.

## 2. PRINTOUT

The most suitable printer is a laser or an inkjet printer. A dot matrix printer should only be used if it possesses an 18 or 24 pin printhead (“letter-quality”).

The printout submitted should be an original; a photocopy is not acceptable. Please make use of good quality plain white A4 (or US Letter) paper size. *The dimensions shown here should be strictly adhered to: do not make changes to these dimensions, which are determined by the document class.* The document class leaves at least 3 cm at the top of the page before the head, which contains the page number.

Printers sometimes produce text which contains light and dark streaks, or has considerable lighting variation either between left-hand and right-hand margins or between text heads and bottoms. To achieve optimal reproduction quality, the contrast of text lettering must be uniform, sharp and dark over the whole page and throughout the article.

If corrections are made to the text, print completely new replacement pages. The contrast on these pages should be consistent with the rest of the paper as should text dimensions and font sizes.

## 3. TABLES AND ILLUSTRATIONS

Tables should be made with  $\text{\LaTeX}$ ; illustrations should be originals or sharp prints. They should be arranged throughout the text and preferably be included *on the same page as they are first discussed*. They should have a self-contained caption and be positioned in flush-left alignment with the text margin. Two small illustrations may be placed alongside one another as shown with Figures 1 and 2. All illustrations will undergo the same reduction as the text.

### 3.1. Tables

Tables should be presented in the form shown in Table 1. Their layout should be consistent throughout.

Table 1

The next-to-leading order (NLO) results *without* the pion field.

$\Lambda$ (MeV)	140	150	175	200
$r_d$ (fm)	1.973	1.972	1.974	1.978
$Q_d$ (fm <sup>2</sup> )	0.259	0.268	0.287	0.302
$P_D$ (%)	2.32	2.83	4.34	6.14
$\mu_d$	0.867	0.864	0.855	0.845
$\mathcal{M}_{M1}$ (fm)	3.995	3.989	3.973	3.955
$\mathcal{M}_{GT}$ (fm)	4.887	4.881	4.864	4.846
$\delta_{1B}^{VP}$ (%)	-0.45	-0.45	-0.45	-0.45
$\delta_{1B}^{C2:C}$ (%)	0.03	0.03	0.03	0.03
$\delta_{1B}^{C2:N}$ (%)	-0.19	-0.19	-0.18	-0.15

The experimental values are given in ref. [4].

Horizontal lines should be placed above and below table headings, above the subheadings and at the end of the table above any notes. Vertical lines should be avoided.

If a table is too long to fit onto one page, the table number and headings should be repeated above the continuation of the table. For this you have to reset the table counter with `\addtocounter{table}{-1}`. Alternatively, the table can be turned by 90° (‘landscape mode’) and spread over two consecutive pages (first an even-numbered, then an odd-numbered one) created by means of `\begin{table}[h]` without a caption. To do this, you prepare the table as a separate L<sup>A</sup>T<sub>E</sub>X document and attach the tables to the empty pages with a few spots of suitable glue.

### 3.2. Useful table packages

Modern L<sup>A</sup>T<sub>E</sub>X comes with several packages for tables that provide additional functionality. Below we mention a few. See the documentation of the individual packages for more details. The packages can be found in L<sup>A</sup>T<sub>E</sub>X’s `tools` directory.

`array` Various extensions to L<sup>A</sup>T<sub>E</sub>X’s `array` and `tabular` environments.

`longtable` Automatically break tables over several pages. Put the table in the `longtable` environment instead of the `table` environment.

`dcolumn` Define your own type of column. Among others, this is one way to obtain alignment on the decimal point.

`tabularx` Smart column width calculation within a specified table width.

`rotating` Print a page with a wide table or figure in landscape orientation using the `sidewaystable` or `sidewaysfigure` environments, and many other rotating tricks. Use the package with the `figuresright` option to make all tables and figures rotate in clockwise. Use the starred form of the `sideways` environments to obtain full-width tables or figures in a two-column article.

### 3.3. Line drawings

Line drawings may consist of laser-printed graphics or professionally drawn figures attached to the manuscript page, correctly aligned. They should be placed either at the bottom or at the top of the page. In the latter case the top of the figure should be at the same level as the first text line.

All notations and lettering should be no less than 2.5 mm high. The use of heavy black, bold lettering should be avoided as this will look unpleasantly dark when printed. Do not use too light or too dark *shading* in your figures. The pages will be reduced to 75–80% of their present size; too dark a shading may become too dense while a very light shading made of tiny points may fade away during reproduction.

### 3.4. PostScript figures

Instead of providing separate drawings or prints of the figures you may also use PostScript files which are included into your L<sup>A</sup>T<sub>E</sub>X file and printed together with the text. Use one of the packages from L<sup>A</sup>T<sub>E</sub>X’s `graphics` directory: `graphics`, `graphicx` or `epsfig`, with the `\usepackage` command, and then use the appropriate commands (`\includegraphics` or `\epsfig`) to include your PostScript file.

Table 2: The next-to-leading order (NLO) results *without* the pion field.

$\Lambda$ (MeV)	140	150	175	200	225	250	Exp.	$v_{18}$ [?]
$r_d$ (fm)	1.973	1.972	1.974	1.978	1.983	1.987	1.966(7)	1.967
$Q_d$ (fm <sup>2</sup> )	0.259	0.268	0.287	0.302	0.312	0.319	0.286	0.270
$P_D$ (%)	2.32	2.83	4.34	6.14	8.09	9.90	–	5.76
$\mu_d$	0.867	0.864	0.855	0.845	0.834	0.823	0.8574	0.847
$\mathcal{M}_{\text{M1}}$ (fm)	3.995	3.989	3.973	3.955	3.936	3.918	–	3.979
$\mathcal{M}_{\text{GT}}$ (fm)	4.887	4.881	4.864	4.846	4.827	4.810	–	4.859
$\delta_{1\text{B}}^{\text{VP}}$ (%)	–0.45	–0.45	–0.45	–0.45	–0.45	–0.44	–	–0.45
$\delta_{1\text{B}}^{\text{C}^2:\text{C}}$ (%)	0.03	0.03	0.03	0.03	0.03	0.03	–	0.03
$\delta_{1\text{B}}^{\text{C}^2:\text{N}}$ (%)	–0.19	–0.19	–0.18	–0.15	–0.12	–0.10	–	–0.21

The experimental values are given in ref. [4].

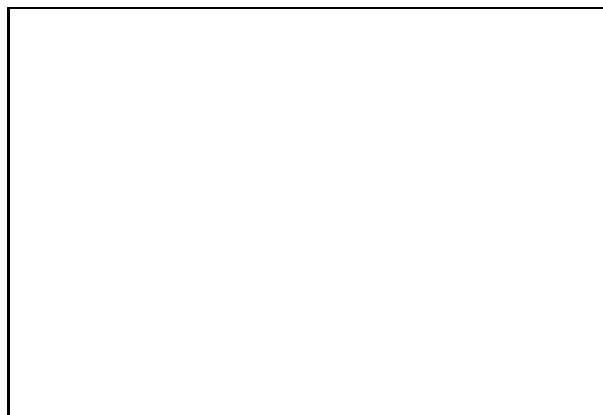


Figure 1. Good sharp prints should be used and not (distorted) photocopies.

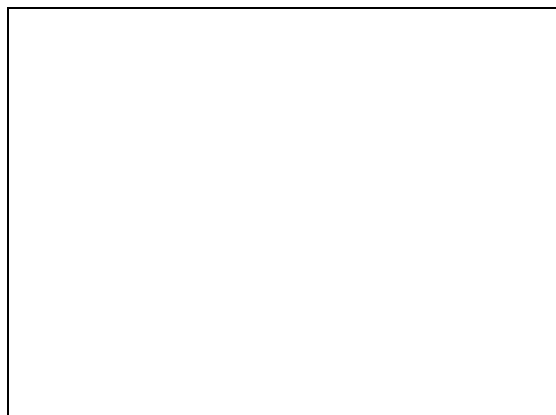


Figure 2. Remember to keep details clear and large enough to withstand a 20–25% reduction.

The simplest command is: `\includegraphics{file}`, which inserts the PostScript file `file` at its own size. The starred version of this command: `\includegraphics*{file}`, does the same, but clips the figure to its bounding box.

With the `graphicx` package one may specify a series of options as a key–value list, e.g.:

```
\includegraphics[width=15pc]{file}
\includegraphics[height=5pc]{file}
\includegraphics[scale=0.6]{file}
\includegraphics[angle=90,width=20pc]{file}
```

See the file `grfguide`, section “Including Graphics Files” of the `graphics` distribution for all options and a detailed description.

The `epsfig` package mimicks the commands familiar from the package with the same name in  $\LaTeX$ 2.09. A PostScript file `file` is included with the command

```
\psfig{file=file}.
```

Grey-scale and colour photographs cannot be included in this way, since reproduction from the printed CRC article would give insufficient typographical quality. See the following subsections.

### 3.5. Black and white photographs

Photographs must always be sharp originals (*not screened versions*) and rich in contrast. They will undergo the same reduction as the text and should be pasted on your page in the same way as line drawings.

### 3.6. Colour photographs

Sharp originals (*not transparencies or slides*) should be submitted close to the size expected in publication. Charges for the processing and printing of colour will be passed on to the author(s) of the paper. As costs involved are per page, care should be taken in the selection of size and shape so that two or more illustrations may be fitted together on one page. Please contact the Author Support Department at Elsevier (E-mail:

authorsupport@elsevier.nl) for a price quotation and layout instructions before producing your paper in its final form.

#### 4. EQUATIONS

Equations should be flush-left with the text margin;  $\text{\LaTeX}$  ensures that the equation is preceded and followed by one line of white space.  $\text{\LaTeX}$  provides the document class option `fleqn` to get the flush-left effect.

$$H_{\alpha\beta}(\omega) = E_{\alpha}^{(0)}(\omega)\delta_{\alpha\beta} + \langle\alpha|W_{\pi}|\beta\rangle \quad (1)$$

You need not put in equation numbers, since this is taken care of automatically. The equation numbers are always consecutive and are printed in parentheses flush with the right-hand margin of the text and level with the last line of the equation. For multi-line equations, use the `eqnarray` environment.

For complex mathematics, use the  $\mathcal{A}\mathcal{M}\mathcal{S}$ math package. This package sets the math indentation to a positive value. To keep the equations flush left, either load the `esprc` package *after* the  $\mathcal{A}\mathcal{M}\mathcal{S}$ math package or set the command `\mathindent=0pt` in the preamble of your article.

#### REFERENCES

1. S. Scholes, Discuss. Faraday Soc. No. 50 (1970) 222.
2. O.V. Mazurin and E.A. Porai-Koshits (eds.), Phase Separation in Glass, North-Holland, Amsterdam, 1984.
3. Y. Dimitriev and E. Kashchieva, J. Mater. Sci. 10 (1975) 1419.
4. D.L. Eaton, Porous Glass Support Material, US Patent No. 3 904 422 (1975).

References should be collected at the end of your paper. Do not begin them on a new page unless this is absolutely necessary. They should be prepared according to the sequential numeric system making sure that all material mentioned is generally available to the reader. Use `\cite` to refer to the entries in the bibliography so that your accumulated list corresponds to the citations made in the text body.

Above we have listed some references according to the sequential numeric system [1–4].

# Inclusive $\pi^0$ spectra at high transverse momentum in d-Au collisions at RHIC

A. Mischke<sup>a\*</sup> for the STAR Collaboration <sup>†</sup>

<sup>a</sup>NIKHEF, Amsterdam, The Netherlands

Preliminary results on inclusive neutral pion production in d-Au collisions at  $\sqrt{s_{\text{NN}}} = 200$  GeV in the pseudo-rapidity range  $0 < \eta < 1$  are presented. The measurement is performed using the STAR Barrel Electromagnetic Calorimeter (BEMC). In this paper, the analysis of the first BEMC hadron measurement is described and the results are compared with earlier RHIC findings. The  $\pi^0$  invariant differential cross sections show good agreement with next-to-leading order (NLO) perturbative QCD calculations.

## 1. Introduction

A suppression of high  $p_T$  hadron production relative to a simple scaling from p-p has been observed in central Au-Au collisions at RHIC [1,2]. It was also found that jet-like correlations opposite to trigger jets are suppressed and that the elliptic anisotropy in hadron emission persists out to very high  $p_T$  [3,4]. In contrast, no suppression effects were seen in d-Au collisions, which provide an important control experiment for the effects of cold nuclear matter. This has led to the conclusion that the observations are due to the high density final state in Au-Au. The most probable explanation to date is parton energy loss from induced gluon radiation (jet quenching). For a recent review see Ref. [5]. To quantitatively understand the existing modification from cold nuclear matter, precise measurements of identified hadrons at high  $p_T$  in d-Au are required. The STAR EMC allows high transverse momentum measurements of  $\pi^0$ ,  $\eta$  mesons and direct photons and may contribute to the identification of  $\rho$  mesons. In this paper we present preliminary results of neutral pion production in d-Au collisions.

## 2. Experimental setup

The results were obtained using two components of the STAR detector system [6], namely the Time Projection Chamber (TPC) and the Barrel Electromagnetic Calorimeter (BEMC). The TPC is situated in a 0.5 Tesla solenoidal magnetic field and provides a precise measurement of the charged particle trajectories. The BEMC [7] is a lead-scintillator sampling calorimeter with a depth of 21 radiation lengths ( $X_0$ ) and an inner radius of 220 cm, divided into towers of granularity  $(\Delta\eta, \Delta\phi) = (0.05, 0.05)$ . Two layers of gaseous shower maximum detectors (SMD), located at a depth of 5  $X_0$ , measure the EM shower shape

\*Present address: Department of Subatomic Physics, University of Utrecht, The Netherlands.

<sup>†</sup>For the full author list and acknowledgments, see Ref. [1].

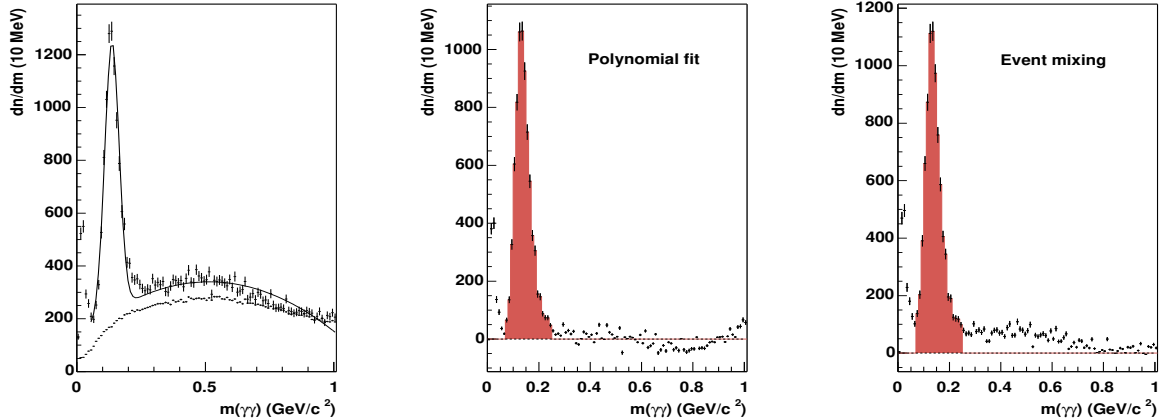


Figure 1. Invariant mass distribution of neutral pion candidates in minimum bias d-Au reactions at  $\sqrt{s_{NN}} = 200$  GeV (left). The solid line is a Gaussian plus second order polynomial fit and the lower histogram is obtained from event mixing. The middle (right) figure is the background subtracted spectrum using the polynomial fit (event mixing). The relative mass resolution is 20%.

with high resolution  $(\Delta\eta, \Delta\phi) = (0.007, 0.007)$ . In this analysis a partial implementation of the BEMC was used, consisting of 2400 towers covering  $0 < \eta < 1$  and full azimuth (the deuteron beam has positive rapidity). When complete, the BEMC will have a coverage of  $-1 < \eta < 1$ . Beam test results [8] provide the absolute energy calibration, whereas the relative calibration is obtained from the peak position of minimum ionizing particles (mostly charged hadrons) on a tower-by-tower basis [9]. Moreover, an overall gain calibration was obtained by comparing the momentum of electrons identified in the TPC with the energy deposited in the BEMC. The achieved energy resolution is  $\delta E/E \approx 16\%/\sqrt{E}$ . In the minimum bias trigger a neutron signal was required in the Zero Degree Calorimeter (ZDC) in the Au beam direction resulting in an acceptance of  $(95 \pm 3)\%$  of the d-Au hadronic cross section. To enhance the high  $p_T$  range, two high tower triggers (HT1 and HT2) were used with an energy threshold of 2.5 GeV and 5 GeV for the highest EMC cluster energy, respectively. The tower occupancy is 1–5% for d-Au events, and the high tower trigger efficiency is nearly 100%.

### 3. Data analysis

After event quality cuts, 10M d-Au events taken in the year 2003 were used for the analysis presented in this paper. Neutral pions were reconstructed in the decay channel  $\pi^0 \rightarrow \gamma\gamma$  (branching fraction 98.8%) by calculating the invariant mass of all pairs of clusters in the calorimeter. Only those clusters were selected which do not have a TPC track pointing to them. Furthermore, a cut on the energy asymmetry was imposed  $|E_1 - E_2|/(E_1 + E_2) \leq 0.5$ . At present, the full calibration of the calorimeter and the finding of noisy and dead towers are in progress. To perform a neutral pion analysis at this stage a sub-sample of good towers was selected. The quality of the individual towers was checked using the  $\pi^0$  invariant mass distribution. The towers are assigned by the decay photons with the highest energy. Only those towers were used which have a well defined  $\pi^0$  signal above the combinatorial background. A Gaussian fit to the  $\pi^0$  signal has



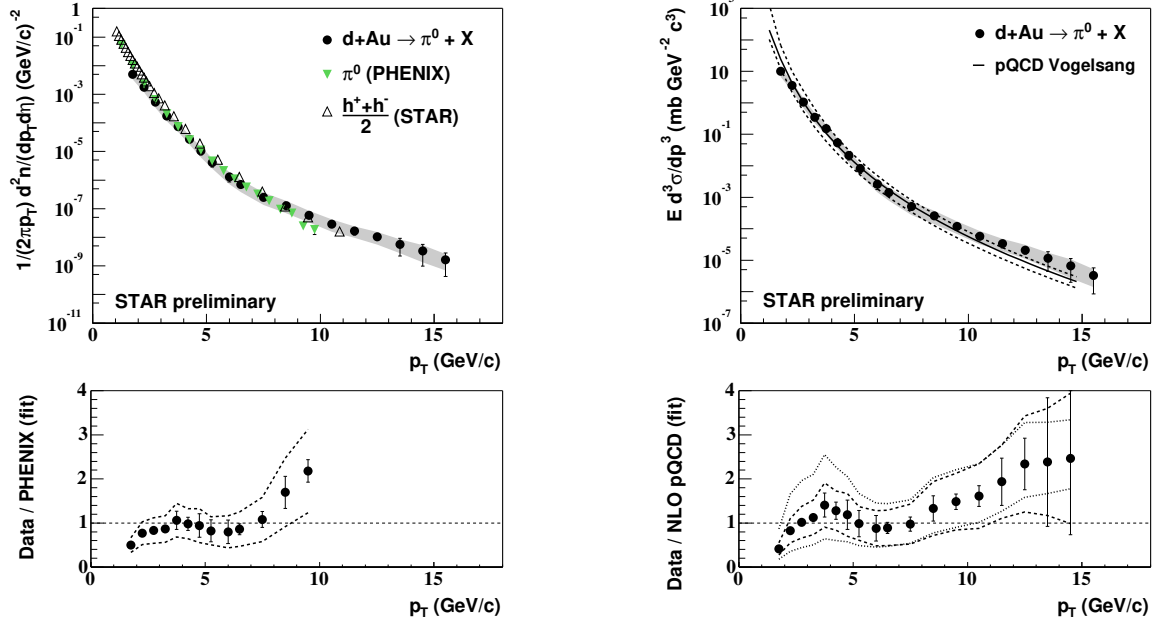


Figure 2. Left: Inclusive  $p_T$  distribution for neutral pions in d-Au collisions at  $0 < \eta < 1$  (solid circles). The error bars (shaded bands) represent the statistical (systematic) uncertainties. Previous STAR measurements on the charged hadron cross section [10] are shown by the open triangles. The full triangles show  $\pi^0$  results from PHENIX [11]. Right: The invariant differential cross section (full circles) compared to NLO pQCD calculations (solid line). The factorization scale uncertainty is illustrated by dashed line. The lower plots show the ratios of the data to a fit of the PHENIX results (left) and to the theory curve (right). The dashed lines indicate the systematic errors derived from the data. The dotted curves (right) were obtained using different factorization scales.

to have a relative mass and width error of 30% and 50%, respectively. By this method approximately one third of all the towers was used for the present analysis. The  $\pi^0$  peak position of all good towers was used to perform an additional tower gain correction (7% on average). In Fig. 1, the resulting invariant mass distribution of cluster pairs is shown. A clear signal is observed with a RMS width of  $28 \text{ MeV}/c^2$ . The combinatorial background from random pairs was estimated by two different methods. First, a second-order polynomial was fitted to the invariant mass distribution outside the peak region (solid curve in the left plot of Fig. 1). The second method describes the background using the event mixing technique. The event mixing distribution, which is shown in the lower histogram in the left plot of Fig. 1, describes the background reasonably well in the range  $0.8\text{--}5 \text{ GeV}/c^2$  (not shown). At lower invariant mass the excess can be attributed to the tail of the  $\pi^0$  peak and a contribution from the  $\eta$  signal ( $m_\eta = 547.3 \text{ MeV}/c^2$ ). The peak observed at  $m < 0.05 \text{ GeV}/c^2$  stems from cluster splittings in the EMC towers.

The background subtracted spectra are shown in the middle and right-hand plot of Fig. 1. The yields per event obtained from both subtraction methods were extracted in  $p_T$  bins (width of  $0.5 \text{ GeV}$  for minimum bias and  $1 \text{ GeV}$  for high tower triggered events) by integrating the background subtracted mass distribution in a range  $\pm 3\sigma$  around the  $\pi^0$  peak. The mean values were used for further analysis and the difference contributes 10–15% to the systematic uncertainties. The signal-to-background ratio increases from 1 at about  $p_T = 1 \text{ GeV}/c$  to 8 at  $4 \text{ GeV}/c$ .

Corrections for reconstruction losses (quality cuts) and detector efficiencies were calculated with Monte-Carlo simulations using the STAR detector geometry and reconstruction software. A correction for the unmeasured trigger fraction, which is expected to be a few percent, is not applied. Losses due to cluster density effects and contributions from weak decays of  $K^0$  mesons are not corrected yet, but are expected to be small. The high tower trigger spectra are normalized using pre-scale factors obtained from the ratios of the BEMC cluster transverse energy distributions in the overlap region. The overall systematic errors related to efficiency, yield extraction, pre-scale factors, and energy calibration are estimated to be 30% for low and 50% for high transverse momenta.

#### 4. Results and discussions

The inclusive  $p_T$  distribution for neutral pions is shown in the left panel of Fig. 2. The yields up to 6 GeV/c are from minimum bias events while above 6 (9.5) GeV/c they are from HT1 (HT2) triggered events. For the different trigger samples the yields have an overlap of one point in the  $p_T$  spectrum and agree within errors. It is seen from Fig. 2 that  $\pi^0$  mesons are presently measured up to  $p_T = 16$  GeV/c. The  $p_T$  spectrum is compared with previous STAR measurements on charged hadron cross section [10] and with PHENIX results on neutral pion production [11]. There is a reasonable agreement within 10–20%.

The right panel of Fig. 2 shows the invariant differential cross sections obtained from the product of the yields and the hadronic cross section in d-Au collisions [10]. The normalization uncertainty is 10%. The results are compared to next-to-leading order (NLO) pQCD predictions [12] which are calculated using the CTEQ6M set of nucleon parton distribution functions [13] and the nuclear parton densities in the gold nucleus from [14]. In this calculation the factorization scale was identified with  $p_T$  and is varied by a factor two to estimate the scale uncertainties (see Fig. 2). The fragmentation functions are taken from [15]. The Cronin effect is not included in the calculations. The data, within errors, are consistent with the calculation up to  $p_T = 15$  GeV/c.

#### REFERENCES

1. J. Adams *et al.* (STAR Collaboration), Phys. Rev. Lett. **92**, 052302 (2004).
2. J. Adams *et al.* (STAR Collaboration), Phys. Rev. Lett. **91**, 172302 (2003).
3. C. Adler *et al.* (STAR Collaboration), Phys. Rev. Lett. **90**, 082302 (2003).
4. C. Adler *et al.* (STAR Collaboration), Phys. Rev. Lett. **90**, 032301 (2003).
5. P. Jacobs and X. N. Wang, to be published in Prog. Part. and Nucl. Phys. (arXiv: hep-ph/0405125).
6. K. H. Ackermann *et al.* (STAR Collaboration), Nucl. Instrum. Meth. **A499**, 624 (2003).
7. M. Beddo *et al.* (STAR Collaboration), Nucl. Instrum. Meth. **A499**, 725 (2003).
8. T. M. Cormier *et al.* (STAR Collaboration), Nucl. Instrum. Meth. **A483**, 734 (2002).
9. J. Adams *et al.* (STAR Collaboration), arXiv: nucl-ex/0407003 (submitted to Phys. Rev. C) .
10. J. Adams *et al.* (STAR Collaboration), Phys. Rev. Lett. **91**, 072304 (2003).
11. S. S. Adler *et al.* (PHENIX Collaboration), Phys. Rev. Lett. **91**, 072303 (2003).
12. W. Vogelsang, 2004, private communication.
13. J. Pumplin *et al.* (CTEQ Collaboration), J. High Energy Phys. **0207**, 012 (2002).
14. L. Frankfurt and M. Strikman, Eur. Phys. J. **A5**, 293 (1999), L. Frankfurt, V. Guzey, M. McDermott, and M. Strikman, J. High Energy Phys. **0202**, 027 (2002), L. Frankfurt, V. Guzey and M. Strikman, arXiv: hep-ph/0303022.
15. B. A. Kniehl, G. Kramer, and B. Pötter, Nucl. Phys. **B582**, 514 (2000).